ARTICLE

Role of the EGF receptor in PPARγ-mediated sodium and water transport in human proximal tubule cells

S. Saad,[1] J. Zhang,[1] R. Yong,[1] D. Yaghobian,[1] M.G. Wong,[1] D.J. Kelly,[2] X.M. Chen,[1] C.A. Pollock[1]

1. Renal Research Laboratories, Kolling Institute of Medical Research, Kolling Building, Royal North Shore Hospital, NSW 2065, Australia

2. Department of Medicine, St Vincent's Hospital, University of Melbourne, Melbourne, Australia

Corresponding author: S. Saad, email sonias@med.usyd.edu.au

Received : 10 November 2012 / Accepted : 4 January 2013

Abstract

Aim/hypothesis This study aimed to determine the interaction between the EGF receptor (EGFR) and peroxisome proliferator-activated receptor γ (PPARγ) and the role of EGFR in sodium and water transport in the proximal tubule.

Methods Primary human proximal tubule cells (PTCs) were exposed to high glucose in the presence and absence of pioglitazone. Total and phospho-EGFR levels and EGFR mRNA expression were determined by western blot and real-time PCR, respectively. Sodium–hydrogen exchanger-3 (NHE3), PPARγ and aquaporin 1 (AQP1) levels were determined by western blot. The role of EGFR was elucidated using the EGFR tyrosine kinase inhibitor, PKI166. The role of PPARγ in high-glucose conditions was determined using specific PPARγ small interfering (si)RNA. P-EGFR, PPARγ, AQP1 and NHE3 production in a rat model of

diabetes (streptozotocin-induced hypertensive Ren-2 transgenic [mRen2]27 rats) and controls, with or without pioglitazone treatment, was determined by immunohistochemistry. The PPARγ and EGFR interaction was determined by chromatin immunoprecipitation assay, and the effect of pioglitazone on EGFR activation by luciferase assay.

Results PTCs exposed to both high glucose and pioglitazone increased protein abundance of P-EGFR, NHE3, AQP1 and PPARγ. Pioglitazone-induced upregulation of NHE3 and AQP1 was abolished by PKI166. High-glucose-induced increases in P-EGFR, NHE3 and AQP1 were decreased with *PPARγ* siRNA. AQP1 and NHE3 but not PPARγ were increased in a diabetic rat model and further increased by pioglitazone treatment. Pioglitazone induced PPARγ binding to the EGFR promoter and subsequent downstream activation.

Conclusions/interpretation Our data suggest that EGFR activation mediates PPARγ-induced sodium and water reabsorption via upregulation of NHE3 and AQP1 channels in the proximal tubule. EGFR inhibition may be a therapeutic strategy in the treatment of diabetic nephropathy and in limiting salt and water retention, which currently restricts the use of PPARγ agonists.

Keywords Diabetic nephropathy, EGF receptor, PPARγ, Sodium retention

Abbreviations

AQP1	Aquaporin-1
ChIP	Chromatin immunoprecipitation
EGFR	EGF receptor
NHE3	Sodium–hydrogen exchanger-3
P-EGFR	Phospho-EGFR
PPARγ	Peroxisome proliferator-activated receptor γ
PTC	Proximal tubular cell

Sgk1	Serum/glucocorticoid kinase receptor
siRNA	Small interfering RNA
t-EGFR	Total EGFR
TZD	Thiazolidinedione

Introduction

Peroxisome proliferator-activated receptor γ (PPARγ) is a member of the nuclear hormone receptor superfamily. Activation of the PPARγ pathway requires heterodimerisation of ligand-bound PPARγ with the retinoid X receptor, which binds specific peroxisome proliferator response elements in the promoter regions of target genes [1]. Despite extensive literature on the beneficial effects of synthetic PPARγ agonists in limiting insulin resistance and protecting pancreatic beta cell function, and our own data suggesting a protective effect on nephropathy [2-5], salt and water retention pose a key limitation to the uptake of these agents in clinical practice.

The proximal tubule mediates 50-75% of total tubular sodium and water reabsorption, with the sodium–hydrogen exchanger-3 (NHE3) and aquaprorin-1 (AQP1) being the key transporter and channel, respectively, mediating transcellular salt and water reabsorption from the tubular ultrafiltrate. We have demonstrated that PPARγ is produced in human proximal tubular cells (PTCs; HK2 cells) and is activated by exposure to high glucose [6], as well as by the insulin-sensitising agents, thiazolidinediones (TZDs) [7]. We have also demonstrated that the serum/glucocorticoid kinase receptor gene, *SGK1*, is a target gene of PPARγ and a mediator for PPARγ agonist-induced NHE3 and AQP1 upregulation in human PTCs [8].

High glucose has been shown to transactivate the EGF receptor (EGFR), and the activation of EGFR through tyrosine phosphorylation occurs in the absence of extracellular ligands in response to PPARγ agonists [9-11]. We have demonstrated that high glucose regulates NHE3 through an EGFR-mediated pathway [11]. This suggests that excessive sodium reabsorption in response to PPARγ activation may occur through regulated downstream activation of EGFR in the proximal tubule. The role of the EGFR in PPARγ-mediated NHE3 and AQP1 production in human PTCs is not known and will be addressed in this study.

Methods

Primary culture of human PTCs Segments of macroscopically and histologically normal renal cortex were obtained under aseptic conditions from patients undergoing nephrectomy for small (<0.06 m) tumours. Patients were accepted for inclusion in the study if there was no history of renal or systemic disease known to be associated with tubulointerstitial pathology. Written informed consent was obtained from each patient before surgery, and ethics approval for the study was obtained from the Royal North Shore Hospital Human Research Ethics Committee. The methods for primary culture of human PTCs are described in detail elsewhere [12]. The ultrastructure, growth and immunohistochemistry of these cells have been well characterised in our laboratory and shown to reproducibly reflect the biology and physiology of their in vivo counterparts [12-14].

Cell culture Human PTCs were grown in 0.1 m tissue culture dishes (Becton Dickinson, North Ryde, NSW, Australia) and exposed to 5 mmol/l D-glucose (control medium), 25 mmol/l D-glucose, 5 mmol/l D-glucose + 20 mmol/l L-glucose (osmotic control) or 10

μmol/l pioglitazone in 5 mmol/l D-glucose for 24 h. L- and D-glucose (ICN Biomedical, Irvine, CA, USA) and pioglitazone (Cayman Chemical, Ann Arbor, MI, USA) were used to determine the specific effects of PPARγ activation. Initial 'dose–response' experiments were undertaken to determine the concentration at which pioglitazone maximally stimulated PPARγ protein expression. On the basis of these studies, we used 10 μmol/l pioglitazone in the experimental protocols as previously described [4, 6, 8]. As pioglitazone is dissolved in DMSO, 0.13% DMSO was used in the control medium for all the pioglitazone-related experiments. The more selective PPARγ agonist, L-805645 (Merck Biosciences, Darmstadt, Germany), was used in some experiments to determine the specific effects of PPARγ activation [8].

To determine the role of EGFR in mediating the observed changes, the EGFR tyrosine kinase inhibitor of the pyrrolopyrimidine class, PKI166 (4 μmol/l), was used as previously described [11], in cells exposed to either high glucose or pioglitazone. PKI166 was synthesised in the laboratories of NIBR (Novartis Institutes for Biomedical Research, North Ryde, NSW, Australia) and was provided by NIBR for the purpose of this study. PKI166 is considered highly specific, with the inhibition constant (IC_{50}) for EGFR being 0.7 nmol/l [15].

Western blotting Western blots were performed on Triton X-100-soluble fractions. PPARγ-specific antibody (Santa Cruz Biotechnology, Santa Cruz, CA, USA), AQP1 and NHE3 antibodies (Chemicon International, Temecula, CA, USA), total EGFR (t-EGFR) antibody (Cell Signaling, Danvers, MA, USA), phospho-EGFR (P-EGFR) antibody (pY1068; Invitrogen, Carlsbad, CA, USA) or actin antibody (Sigma-Aldrich, St Louis, MO, USA) were used overnight followed by incubation with anti-rabbit or anti-mouse

antibody (Amersham Pharmaceuticals, Rydalmere, NSW, Australia) for 1 h at room temperature. Data were normalised to actin to ensure equal protein loading. The bands corresponding to AQP1 (28 kDa), PPARγ (67 kDa), NHE3 (85 kDa), t-EGFR or P-EGFR (170 kDa) and actin (42 kDa) were quantified using NIH Image software version 1.60.

Real-time RT-PCR RNA was extracted using an RNeasy Mini Kit (Qiagen, Valencia, CA, USA) according to the manufacturer's instructions. cDNA was generated by reverse transcribing 1 μg total RNA in a reaction volume of 20 μl using VILO cDNA Synthesis Kits (Invitrogen). Sequence-specific primers for human EGFR and β-actin are described in electronic supplementary material (ESM) Table 1. Primer specificity in real-time PCRs was confirmed using RT-PCR. A 25 μl real-time PCR included Brilliant SYBR Green QRT–PCR Master Mix according to the manufacturer's instructions (Stratagene, La Jolla, CA, USA). Quantitative real-time PCR was performed using an ABI Prism 7,900 HT Sequence Detection System (Applied Biosystems, Mulgrave, VIC, Australia). Reactions were performed in at least triplicate and analysed by relative quantification using RQ Manager software, version 1.2 (Applied Biosystems). All data are presented as fold change compared with control after normalisation to the housekeeping gene, β-actin.

PPARγ silencing Small interfering RNA (siRNA) was designed to specifically target *PPARγ* mRNA sites. *PPARγ* siRNA target is as follows: GCCTCATGAAGAGCCTTCCAACTCCCTCA (Ambion, Mulgrave, VIC, Australia). PTCs were transfected with 8 nmol/l *PPARγ* siRNA using Ribojuice (Novagen, Madison, WI, USA) as per the manufacturer's instructions. Protein levels were determined using western blot. All siRNA experiments included non-specific control (*NSC* siRNAs; Ambion). Once PPARγ knockdown was confirmed, subsequent experiments were

conducted to determine the effect of exposure to high glucose (25 mmol/l) on AQP1, NHE3 and P-EGFR levels 24 h after PPARγ knockdown. Cell lysates were then collected. Western blotting experiments were performed as described above.

In vivo experiments To determine P-EGFR levels in an in vivo model of diabetes mellitus, we used the streptozotocin-induced hypertensive Ren-2 transgenic rat (mRen2)27 rat model. These animals were confirmed to have demonstrable hyperfiltration, proteinuria and pathological signs of diabetic nephropathy at the time of study. This model has been previously validated for studies in diabetic nephropathy [16-20]. Briefly, 6-week-old female, heterozygous Ren-2 rats, weighing 0.125±5 kg, were randomised to receive either 55 mg/kg streptozotocin (STZ; Sigma) (diabetic) or buffer alone (non-diabetic) by tail vein injection after an overnight fast. Diabetic Ren-2 rats were subsequently treated with 5 mg/kg pioglitazone (Cayman Chemical) fed by gavage or sham treatment for 12 weeks starting 7 days after STZ injection. Experimental procedures adhered to the guidelines of the National Health and Medical Research Council of Australia's Code for the care and use of animals for scientific purposes and have been approved by St Vincent's Hospital Animal Ethics Committee, Melbourne, Australia. Serial sections of 4 μmol/l thickness were fixed in 4% paraformaldehyde, and paraffin sections were prepared for immunohistochemistry. Levels of P-EGFR, PPARγ, NHE3 and AQP1 protein were determined.

Immunohistochemistry Paraffin-embedded sections were dewaxed in xylene and rehydrated in graded concentrations of ethanol. Endogenous peroxidase activity was blocked by immersion in 3% H_2O_2 for 5 min. Epitope retrieval was required for P-EGFR, AQP1 and NHE3, but not PPARγ, staining. Heat retrieval was performed in 0.01 mol/l

citrate buffer, pH 6.0, using a pressure cooker set at 121°C for 30 s. Non-specific protein binding was blocked with a protein block (Dako, Troy, MI, USA). Incubation with primary antibodies was performed using a Sequenza vertical cover-plate immunostaining system (Thermofisher Scientific, Scoresby, VIC, Australia) using 0.2 μg P-EGFR (Tyr1173) antibody, 4 μg PPARγ antibody (both from Santa Cruz), 0.2 μg NHE3 antibody (Novus Biologicals, Littleton, CO, USA) or 4 μg AQP1 antibody (Santa Cruz) overnight at 4°C. The primary antibodies were subsequently localised using biotinylated secondary anti-mouse or anti-rabbit IgG antibodies. Horseradish peroxidase-conjugated streptavidin was subsequently used to visualise the tissue immune complexes using the LSAB+ detection system (Dako). Antigen–antibody reactions were visualised with the chromogen, diaminobenzidine, and counterstaining was performed using Mayer's Haematoxylin followed by Scott's Blue staining (Fronine, Taren Point, NSW, Australia). Control sections were also prepared in which the authentic primary antibodies were replaced with an irrelevant isotype-matched IgG. The tissue specimens were examined by bright field microscopy using a Leica photomicroscope linked to a DFC 480 digital camera.

Quantification of histological variables In brief, 10 random non-overlapping fields from three stained sections were captured and digitised using an AxioImager.A1 microscope (Carl Zeiss AxioVision, Kirchdorf, Germany) attached to an AxioCam MRc5 digital camera (Carl Zeiss AxioVision). Areas of brown staining reflecting P-EGFR, PPARγ, AQP1 or NHE3 production were quantified and calculation of the proportional area stained brown was then determined using image analysis software AIS (Analytic Imaging Station version 6.0, Imaging Research, St Catherines, ON, Canada).

Chromatin immunoprecipitation assay A chromatin immunoprecipitation (ChIP) assay was performed using an EZ ChIP Kit (Millipore, Billerica, MA, USA) according to the manufacturer's instructions. In brief, cells were crosslinked in 1% formaldehyde after different cell culture treatments. Cells were then lysed and sonicated. Sonication was optimised to achieve 200 to 1000 bp DNA fragments. Equal amounts of protein were incubated with 4 μg/ml PPARγ antibody (Santa Cruz Biotechnology). The crosslink of immunoprecipitated protein–DNA samples was then reversed, and DNA samples were purified using spin columns. PPARγ-binding sites of the *EGFR* promoter were quantified using real-time PCR. Primers used for the promoter region are described in ESM Table 2.

EGFR promoter activity assay The promoter activity of *EGFR* was determined by the Dual-Luciferase Reporter Assay System (Promega, Madison, WI, USA) as we have described previously [21]. In brief, the DNA fragment (1,900 bp) of the *EGFR* promoter was amplified using PfuUltra II HS Fusion DNA Polymerase (Agilent Technologies, Santa Clara, CA, USA). The DNA fragment of the *EGFR* promoter containing the PPARγ-binding site (−1271: AGGTCCTAGTGAA) was subcloned into pGL3 firefly luciferase vector (Promega). The plasmid, pGL3-*EGFR* promoter, or the pGL3 basal plasmid was introduced into PTCs using Lipofectamine 2000 (Invitrogen). pRL-SV40 *Renilla* vector (Promega) was cotransfected into cells, and its luciferase activity was used for normalisation of transfection efficiency. Cells were then exposed to pioglitazone or L-805645 for 24 h, and luciferase activity was detected by POLARstar (BMG Labtech, Offenburg, Germany).

Statistical analysis Results are expressed as a percentage or fold change compared with the control. Experiments were performed in at least three different culture preparations

derived from each patient, and at least three data points for each experimental condition were measured in each preparation. Six animals in each group were used in the in vivo study. Results are expressed as mean±SEM, with *n* reflecting the number of culture preparations. Statistical comparisons between groups were made by ANOVA, with pairwise multiple comparisons made by Fisher's protected least significant difference test. Analyses were performed using the software package, Statview version 4.5 (Abacus Concepts, Piscataway, NJ, USA). p values ≤ 0.05 were considered significant.

Results

High glucose and pioglitazone induce PPARγ We have previously demonstrated that high glucose and pioglitazone increase PPARγ protein expression in human PTCs (HK2 cells) [6]. We have confirmed that PPARγ protein content was significantly increased to 199±21.6% in human primary PTCs when exposed to 25 mmol/l glucose (HG) (p<0.05). Exposure to the osmotic control (OC) had no effect on PPARγ levels (109±23.4%; p=0.7) (Fig. 1a). Exposure to 10 μmol/l pioglitazone also increased PPARγ protein levels to 142±6.2% (p<0.01) (Fig. 1b).

Combined effect of high glucose and pioglitazone on EGFR High glucose increased t-EGFR levels to 414±150% of control, most of which (360±2%) was phosphorylated (p<0.05 vs control) (Fig. 2a, b). P-EGFR is produced at low levels in human PTCs, as we have previously described [11] and as is also shown in Fig. 5. The combination of high glucose and pioglitazone increased t-EGFR protein content to 1102±329% (p<0.01), in addition to increasing EGFR phosphorylation to 575±89% (p<0.001) (Fig. 2a, b). High glucose in the absence and presence of pioglitazone increased *EGFR* mRNA levels to1.3±0.03-fold (p<0.001) and 1.7±0.1-fold (p<0.01), respectively (Fig. 2c).

Pioglitazone increases NHE3 and AQP1 through an EGFR pathway We have confirmed that NHE3 is significantly increased when PTCs are exposed to pioglitazone, as we have previously demonstrated [8], to 167±16.1% (p<0.01). To determine the role of EGFR in increased NHE3 production, we exposed cells to the EGFR tyrosine kinase inhibitor, PKI166, in the presence of pioglitazone, and NHE3 protein content was assessed. The combination of PKI166 with pioglitazone abrogated the observed increase in NHE3

levels with the PPARγ agonist, pioglitazone, to 103±6.1% (Fig. 3a). These results suggest that the upregulation of NHE3 after exposure to pioglitazone is EGFR mediated.

As we have previously demonstrated [8], pioglitazone significantly increased AQP1 protein production to 201±23% of control values (p<0.01). The combination of PKI166 with pioglitazone abrogated the observed increase in AQP1 levels with the PPARγ agonist, pioglitazone, to 95±21% (p= 0.7 vs control) (Fig. 3b). These results suggest that the upregulation of AQP1 after exposure to pioglitazone is also mediated through the EGFR.

High-glucose-induced P-EGFR, NHE3 and AQP1 is PPARγ mediated Since pioglitazone has PPARγ-mediated and PPARγ-independent effects, to demonstrate the specific role of PPARγ in the high-glucose-mediated increase in P-EGFR, we performed experiments in the presence of specific *PPARγ* siRNA. As clearly demonstrated, we were able to significantly block PPARγ protein expression using specific *PPARγ* siRNA to 27±4% of control values (p<0.001) (Fig. 4a). Phosphorylation of EGFR after high glucose exposure was confirmed using immunoprecipitation. High glucose significantly induced P-EGFR to 120.5±1.5% (p<0.01). This increase was abolished in the presence of *PPARγ* siRNA to 96.5±9.5% (Fig. 4b). This suggests that the effect of pioglitazone on P-EGFR is PPARγ mediated.

To confirm that the high-glucose effect on NHE3 and AQP1 is PPARγ mediated, we repeated experiments in the presence of *PPARγ* siRNA. High-glucose-induced increases in NHE3 and AQP1 levels were significantly inhibited to basal levels in the presence of *PPARγ* siRNA (to 91±17% and 78±12.8%, respectively) (Fig. 4c, d). These data show that the high-glucose increase in NHE3 and AQP1 in human PTCs is PPARγ mediated.

Effect of high glucose and pioglitazone on P-EGFR, AQP1, NHE-3 and PPARγ levels in vivo The expression of P-EGFR and the effect of high glucose and pioglitazone on P-EGFR expression in the proximal tubule were confirmed in an in vivo model of diabetes mellitus. P-EGFR levels were very low in the proximal tubule of non-diabetic rats. However, its levels were increased in the proximal tubule membranes and cytoplasm of diabetic rats and further increased in diabetic rats treated with pioglitazone (Fig. 5). As expected, nuclear and cytoplasmic abundance of PPARγ was shown in control rats (Fig. 6a). However, this was decreased in the diabetic rats. Interestingly only cytoplasmic staining of PPARγ was shown in the diabetic rats (Fig. 6b). In diabetic rats, cytoplasmic and nuclear PPARγ levels were significantly increased in the presence of pioglitazone (Fig. 6c), suggesting increased PPARγ activity. NHE3 is found at a low level in the tubules of control rats (Fig. 7a). Its levels were more concentrated in the luminal membrane of the tubule. This was increased in the diabetic rats and further increased in the presence of pioglitazone with increased perinuclear staining (Fig. 7b, c). Similarly, increased levels of AQP1 were demonstrated in the diabetic rats compared with controls (Fig. 8a, b). AQP1 is clearly produced in the luminal membrane of the tubules. Its content was significantly increased in the presence of pioglitazone. Interestingly, pioglitazone also increased AQP1 levels in the apical brush border as well as in the luminal membrane (Fig. 8c).

PPARγ regulates EGFR expression and activity by binding to EGFR promoter, and thiazolidinediones promote this binding Using a motif scan program, we determined that the *EGFR* promoter contains a PPARγ-binding site at −1271: AGGTCCTAGTGAA. The ability of PPARγ to bind the *EGFR* promoter was tested using a ChIP assay. The data

show that pioglitazone significantly increased PPARγ binding to the *EGFR* promoter 1.66± 0.2-fold (p<0.05) (Fig. 9a). In addition, the more selective PPARγ agonist, L-805645, further increased PPARγ–*EGFR* promoter binding 8.8±2.6-fold (p<0.05) (Fig. 9a). This suggests that PPARγ can bind to the *EGFR* promoter to regulate its transcriptional activity.

Since PPARγ can directly bind the *EGFR* promoter, and in order to establish if this binding induces EGFR activation, we determined the promoter activity of *EGFR* after PPARγ activation by a Dual-Luciferase Reporter Assay. Pioglitazone increased luciferase activity 1.5±0.1-fold (p<0.05), and L-805645 further increased luciferase activity 5.5±1.5-fold (p<0.05) (Fig. 9b).

Discussion

Cellular sodium and water transport are dysregulated in patients with diabetes mellitus, which are considered to be at least in part responsible for the high incidence of hypertension observed in these patients. EGFR is activated/transactivated by EGF, high glucose and angiotensin II, all factors implicated in the pathogenesis of diabetic nephropathy. To date, only a few studies have focused on the role of EGFR in enhancing tubular fluid reabsorption in the kidney proximal tubule. We have demonstrated that high glucose transactivates EGFR, which then regulates the key transporter of proximal tubular sodium reabsorption, NHE3, through downstream regulation of Sgk1 [11]. In addition, we have shown that NHE3 is regulated through Sgk1 by TZDs [8]. The possible role of EGFR in the TZD-mediated effects on sodium and water retention in the proximal tubule was examined in the present study. We have confirmed that PPARγ is produced in human PTCs and its level is increased after exposure to high glucose and the clinically

available PPARγ ligand (pioglitazone). This is consistent with our previous findings using the HK2 primary human PTC line [6]. We have also confirmed, using in vivo models of STZ-induced diabetes mellitus, that PPARγ is produced in the proximal tubule and upregulated in diabetic animals in the presence of pioglitazone. Interestingly, diabetic animals had reduced levels of nuclear PPARγ. Our data show that, in diabetic animals, PPARγ nuclear translocation was diminished, suggesting reduced PPARγ activity, as has been previously reported [22]. In addition, we have specifically determined that a combination of high glucose with pioglitazone increased total *EGFR* mRNA and protein expression and EGFR phosphorylation. Although high glucose increased P-EGFR levels, there was no change in *EGFR* mRNA levels. In vivo*,* diabetic Ren-2 rats also showed increased P-EGFR expression, which was further potentiated by treatment with pioglitazone.

One of the most important functions of the kidney is to maintain electrolyte and metabolic homeostasis. Our results show that blockade of EGFR phosphorylation using PKI166, a novel and highly specific EGFR tyrosine kinase inhibitor of the pyrrolopyrimidine class, attenuates the increased abundance of NHE3 and AQP1 in PTCs in response to pioglitazone. This novel finding suggests a role for EGFR in TZD-mediated sodium and water transport in the proximal tubule. Drumm et al have demonstrated that aldosterone-induced NHE3 cell surface expression and activity in the proximal tubule is EGFR-dependent [23]. EGFR activation leads to a specific decrease in the levels of the tight junction integral protein, claudin-2, which results in modulation of paracellular sodium transport in MDCK cells [24, 25]. Under physiological conditions, EGFR activation appears to play an important role in the regulation of renal

haemodynamics and electrolyte handling by the kidney, whereas, in different pathophysiological states, EGFR activation may mediate either beneficial or detrimental effects on the kidney [26]. The interdependence of PPARγ and EGFR in the kidney has not been previously shown. However, in other tissues such as cancer and endothelial cells, EGFR is modulated by PPARγ agonists in a PPARγ-dependent and -independent manner.

To determine if the high-glucose effect on NHE3 and AQP1 is PPARγ mediated, we used *PPARγ* siRNA. Our data show that P-EGFR is regulated downstream of PPARγ in response to high glucose. We have shown that high-glucose-induced P-EGFR is PPARγ mediated, and the high-glucose-mediated increase in NHE3 and AQP1 is also through PPARγ. In addition, we have clearly demonstrated that NHE3 and AQP1 are increased in diabetic rats and further increased in the presence of pioglitazone and that pioglitazone increased AQP1 expression in the brush border. Increased levels of NHE3 and AQP1 represent increased activity, as previously described [8, 27]. This explains at least in part the enhanced salt and water retention observed with pioglitazone use in patients with diabetes mellitus. Our data suggests cross-talk between PPARγ and EGFR in human PTCs. PPARγ and EGFR signalling is known to intersect in some cell types. For example, PPARγ regulation of urothelial differentiation is modulated by downstream EGFR signalling [28]. Coordinated activity between PPARγ and EGFR has been documented in the induction of caveolin-1 by rosiglitazone treatment in human colon cancer cells [29]. Interestingly, Lewis et al have recently reported that patients treated with pioglitazone have an increased risk of urinary bladder cancer if the drug is taken for

more than 2 years and at a high dose [30]. The risk of increased bladder cancer is potentially mitigated by the use of EGFR inhibitors.

We have uniquely demonstrated that *EGFR* has a PPARγ-binding site and that TZD not only increased PPARγ levels but also its binding to the *EGFR* promoter and EGFR activation. Our findings suggest that high glucose and TZDs activate/transactivate PPARγ, which, through direct binding and downstream activation of EGFR, then induce NHE3 and AQP1 in the proximal tubule. Hence, the abnormalities in tubular cell growth known to occur in diabetic nephropathy, cellular sodium and water transport which are dysregulated in diabetes mellitus, and the increase in sodium reabsorption known to be responsible for the observed fluid retention with the use of TZDs are likely to occur through an EGFR-dependent mechanism. These data clearly highlight the importance of EGFR in renal sodium reabsorption and suggest that PPARγ agonists in combination with the clinically available EGFR blockers may be beneficial in regulating the nephromegaly and excessive sodium reabsorption observed in diabetic nephropathy. In fact, EGFR tyrosine kinase inhibition ameliorates the early changes that occur in diabetic nephropathy such as tubular epithelial cell proliferation, glomerular enlargement and changes in kidney weight in diabetic rats [31] and suppresses TGFβ-mediated matrix protein production in rat kidney interstitial fibroblasts [32]. Diabetic rats administered an EGFR tyrosine kinase inhibitor showed attenuated kidney and glomerular enlargement and a reduction in albuminuria, in association with podocyte preservation [31, 33]. These studies, in addition to our data, suggest that inhibition of the EGFR may provide an attractive therapeutic target for the treatment of diabetic nephropathy as well as limiting salt and water retention, which currently restricts the use of PPARγ agonists.

Acknowledgements

We acknowledge the support of the Department of Urology of Royal North Shore Hospital and Concord Hospital for assisting in procuring the kidneys for primary culture. We would like to thank S. Smith (Raymond Purves Bone and Joint Research Laboratories, Kolling Institute for Medical Research, Australia) for help with immunohistochemistry experiments and S. Kurdukov (Functional Genomics, Kolling Institute of Medical Research, Australia) for help with quantification of histological variables.

Funding

This study was partly supported by the National Health and Medical Research Council of Australia and the Staff Specialist Research Grant (Ramsay Healthcare Foundation).

Duality of interest

The authors declare that there is no duality of interest associated with this manuscript.

Contribution statement

SS contributed to the study design, data collection, analysis and interpretation of results and wrote the manuscript. JZ, RY and DY performed experiments, analysed data and contributed to the revision of the article. MGW provided technical support and contributed to the acquisition of data and revision of the article. XMC and DJK contributed to the study design, interpretation of results and manuscript revision. CAP contributed to the study design, interpretation of results, manuscript drafting and revision. All authors approved the final version of the article.

References

[1] Miyata KS, McCaw SE, Marcus SL, Rachubinski RA, Capone JP (1994) The peroxisome proliferator-activated receptor interacts with the retinoid X receptor in vivo. Gene 148: 327-330.

[2] Panchapakesan U, Chen XM, Pollock CA (2005) Drug insight: thiazolidinediones and diabetic nephropathy–relevance to renoprotection. Nat Clin Pract Nephrol 1: 33-43

[3] Panchapakesan U, Sumual S, Pollock CA, Chen X (2005) PPARgamma agonists exert antifibrotic effects in renal tubular cells exposed to high glucose. Am J Physiol Renal Physiol 289: F1153-1158

[4] Zafiriou S, Stanners SR, Polhill TS, Poronnik P, Pollock CA (2004) Pioglitazone increases renal tubular cell albumin uptake but limits proinflammatory and fibrotic responses. Kidney Int 65: 1647-1653

[5] Zafiriou S, Stanners SR, Saad S, Polhill TS, Poronnik P, Pollock CA (2005) Pioglitazone inhibits cell growth and reduces matrix production in human kidney fibroblasts. J Am Soc Nephrol 16: 638-645

[6] Panchapakesan U, Pollock CA, Chen XM (2004) The effect of high glucose and PPAR-gamma agonists on PPAR-gamma expression and function in HK-2 cells. Am J Physiol Renal Physiol 287: F528-534

[7] Izzedine H, Launay-Vacher V, Buhaescu I, Heurtier A, Baumelou A, Deray G (2005) PPAR-gamma-agonists' renal effects. Minerva Urol Nefrol 57: 247-260

[8] Saad S, Agapiou DJ, Chen XM, Stevens V, Pollock CA (2009) The role of Sgk-1 in the upregulation of transport proteins by PPAR-{gamma} agonists in human proximal tubule cells. Nephrol Dial Transplant 24: 1130-1141

[9] Gardner OS, Dewar BJ, Earp HS, Samet JM, Graves LM (2003) Dependence of peroxisome proliferator-activated receptor ligand-induced mitogen-activated protein kinase signaling on epidermal growth factor receptor transactivation. J Biol Chem 278: 46261-46269

[10] Slomiany BL, Slomiany A (2004) Role of epidermal growth factor receptor transactivation in PPAR gamma-dependent suppression of Helicobacter pylori interference with gastric mucin synthesis. Inflammopharmacology 12: 177-188

[11] Saad S, Stevens VA, Wassef L, et al. (2005) High glucose transactivates the EGF receptor and up-regulates serum glucocorticoid kinase in the proximal tubule. Kidney Int 68: 985-997

[12] Johnson DW BB, Poronnik P, Cook DI, Field MJ and Pollock CA (1997) Transport characteristics of human proximal tubule cells in primary culture. Nephrology 3: 183-194

[13] Johnson DW, Saunders HJ, Brew BK, et al. (1997) Human renal fibroblasts modulate proximal tubule cell growth and transport via the IGF-I axis. Kidney Int 52: 1486-1496

[14] Qi W, Johnson DW, Vesey DA, Pollock CA, Chen X (2007) Isolation, propagation and characterization of primary tubule cell culture from human kidney. Nephrology (Carlton) 12: 155-159

[15] Bruns CJ, Solorzano CC, Harbison MT, et al. (2000) Blockade of the epidermal growth factor receptor signaling by a novel tyrosine kinase inhibitor leads to apoptosis of endothelial cells and therapy of human pancreatic carcinoma. Cancer Res 60: 2926-2935

[16] Kelly DJ, Cox AJ, Tolcos M, Cooper ME, Wilkinson-Berka JL, Gilbert RE (2002) Attenuation of tubular apoptosis by blockade of the renin-angiotensin system in diabetic Ren-2 rats. Kidney Int 61: 31-39

[17] Kelly DJ, Wilkinson-Berka JL, Gilbert RE (2007) Progressive diabetic nephropathy in the Ren-2 rat. Am J Physiol Renal Physiol 292: F1662; author reply F1663

[18] Kelly DJ, Stein-Oakley A, Zhang Y, et al. (2004) Fas-induced apoptosis is a feature of progressive diabetic nephropathy in transgenic (mRen-2)27 rats: attenuation with renin-angiotensin blockade. Nephrology (Carlton) 9: 7-13

[19] Wilkinson-Berka JL, Kelly DJ, Koerner SM, et al. (2002) ALT-946 and aminoguanidine, inhibitors of advanced glycation, improve severe nephropathy in the diabetic transgenic (mREN-2)27 rat. Diabetes 51: 3283-3289

[20] Qi W, Chen X, Holian J, Tan CY, Kelly DJ, Pollock CA (2009) Transcription factors Kruppel-like factor 6 and peroxisome proliferator-activated receptor-{gamma} mediate high glucose-induced thioredoxin-interacting protein. Am J Pathol 175: 1858-1867

[21] Qi W, Chen X, Gilbert RE, et al. (2007) High glucose-induced thioredoxin-interacting protein in renal proximal tubule cells is independent of transforming growth factor-beta1. Am J Pathol 171: 744-754

[22] Shibuya A, Wada K, Nakajima A, et al. (2002) Nitration of PPARgamma inhibits ligand-dependent translocation into the nucleus in a macrophage-like cell line, RAW 264. FEBS Lett 525: 43-47

[23] Drumm K, Kress TR, Gassner B, Krug AW, Gekle M (2006) Aldosterone stimulates activity and surface expression of NHE3 in human primary proximal tubule epithelial cells (RPTEC). Cell Physiol Biochem 17: 21-28

[24] Singh AB, Harris RC (2004) Epidermal growth factor receptor activation differentially regulates claudin expression and enhances transepithelial resistance in Madin-Darby canine kidney cells. J Biol Chem 279: 3543-3552

[25] Singh AB, Sugimoto K, Harris RC (2007) Juxtacrine activation of epidermal growth factor (EGF) receptor by membrane-anchored heparin-binding EGF-like growth factor protects epithelial cells from anoikis while maintaining an epithelial phenotype. J Biol Chem 282: 32890-32901

[26] Zeng F, Singh AB, Harris RC (2009) The role of the EGF family of ligands and receptors in renal development, physiology and pathophysiology. Exp Cell Res 315: 602-610

[27] Stevens VA, Saad S, Poronnik P, Fenton-Lee CA, Polhill TS, Pollock CA (2008) The role of SGK-1 in angiotensin II-mediated sodium reabsorption in human proximal tubular cells. Nephrol Dial Transplant 23: 1834-1843

[28] Varley CL, Southgate J (2008) Effects of PPAR agonists on proliferation and differentiation in human urothelium. Exp Toxicol Pathol 60: 435-441

[29] Tencer L, Burgermeister E, Ebert MP, Liscovitch M (2008) Rosiglitazone induces caveolin-1 by PPARgamma-dependent and PPRE-independent mechanisms: the role of EGF receptor signaling and its effect on cancer cell drug resistance. Anticancer Res 28: 895-906

[30] Lewis JD, Ferrara A, Peng T, et al. (2011) Risk of bladder cancer among diabetic patients treated with pioglitazone: interim report of a longitudinal cohort study. Diabetes Care 34: 916-922

[31] Wassef L, Kelly DJ, Gilbert RE (2004) Epidermal growth factor receptor inhibition attenuates early kidney enlargement in experimental diabetes. Kidney Int 66: 1805-1814

[32] Kang JH, Cho HJ, Lee IS, Kim M, Lee IK, Chang YC (2009) Comparative proteome analysis of TGF-beta1-induced fibrosis processes in normal rat kidney interstitial fibroblast cells in response to ascofuranone. Proteomics 9: 4445-4456

[33] Advani A, Wiggins KJ, Cox AJ, Zhang Y, Gilbert RE, Kelly DJ (2011) Inhibition of the epidermal growth factor receptor preserves podocytes and attenuates albuminuria in experimental diabetic nephropathy. Nephrology (Carlton) 16: 573-581

Fig. 1 High glucose and pioglitazone induce PPARγ protein expression. PTCs were incubated for 24 h with 5 mmol/l glucose medium (Control), 25 mmol/l glucose (HG), 5 mmol/l glucose medium with 20 mmol/l glucose (osmotic control; OC) or 10 μmol/l pioglitazone (Piog) in control medium. Representative western blotting images are shown for PPARγ and actin bands after high-glucose (**a**) or pioglitazone (**b**) exposure. Normalised results are expressed as mean±SEM (n=3). *p<0.05 and **p<0.01 vs control

Fig. 2 Effect of high glucose in the presence and absence of pioglitazone on EGFR. PTCs were incubated for 24 h with 5 mmol/l glucose medium (Control) in the presence or absence of pioglitazone (Piog), and levels of P-EGFR were quantified.

Representative western blotting images for t-EGFR (**a**) and P-EGFR (**b**) are shown. *EGFR* mRNA expression is shown in (**c**). Normalised results are expressed as mean±SEM (n=3). *p<0.05, **p<0.01 and ***p<0.001 vs control and $^{\dagger}p$<0.05 vs HG

Fig. 3 PPARγ agonist-induced increase in NHE3 and AQP1 is P-EGFR mediated. PTCs were incubated for 24 h with 5 mmol/l glucose medium (Control) or pioglitazone (Piog) with or without PKI166 (4 μmol/l), and levels of NHE3 (**a**) or AQP1 (**b**) were determined by western blotting. Representative images for NHE3, AQP1 and actin bands are shown. Normalised results are expressed as mean±SEM (n=4). **p<0.01 vs control

Fig. 4 High-glucose-induced increase in P-EGFR, NHE3 and AQP1 is PPARγ mediated. Decreased content of PPARγ was confirmed in gene-silenced PTCs using *PPARγ* siRNA vs *non-specific* siRNA control (*NSC*) (**a**). PTCs were incubated for 24 h with 5 mmol/l glucose medium (Control) or high glucose (HG) in the presence of *PPARγ* siRNA or *NSC* siRNA. P-EGFR (**b**), NHE3 (**c**) or AQP1 (**d**) protein content was determined by western blotting. Representative images for P-EGFR, NHE3, AQP1 and

actin bands are shown. Normalised results are expressed as mean±SEM (n=3). *p<0.05, **p<0.01 and ***p<0.001 vs *NSC* siRNA

Fig. 5 P-EGFR levels in diabetic rats with and without pioglitazone (Piog). Immunohistochemistry of P-EGFR in control Ren-2 rats (**a**) and diabetic (**b**) and diabetic+pioglitazone-treated (**c**) animals. Negative IgG was performed to confirm staining specificity (not shown). Magnification ×400. Quantification of P-EGFR immunostaining is shown (**d**). Values are represented as mean±SEM. ***p<0.001 and ****p<0.0001 vs control and $^{\dagger\dagger}p$<0.01 vs diabetic

Fig. 6 PPARγ levels in diabetic rats with and without pioglitazone (Piog). Immunohistochemistry of PPARγ in control Ren-2 rats (**a**) and diabetic (**b**) and diabetic+pioglitazone-treated (**c**) animals. Negative IgG was performed to confirm staining specificity (not shown). Magnification ×400. Quantification of PPARγ immunostaining is shown (**d**). Values are represented as mean±SEM. *p<0.05 vs control and $^{\dagger\dagger}p$<0.01 vs diabetic

Fig. 7 NHE3 levels in diabetic rats with and without pioglitazone (Piog). Immunohistochemistry of NHE3 in control Ren-2 rats (**a**) and diabetic (**b**) and diabetic+pioglitazone-treated (**c**) animals. Negative IgG was performed to confirm staining specificity (not shown). Magnification ×400. Quantification of NHE3 immunostaining is shown (**d**). Values are represented as mean±SEM. **p<0.01 and ***p<0.001 vs control and $^{\dagger}p$<0.05 vs diabetic

Fig. 8 AQP1 expression in diabetic rats with and without pioglitazone (Piog). Immunohistochemistry of AQP1 in control Ren-2 rats (**a**) and diabetic (**b**) and diabetic+pioglitazone-treated (**c**) animals. Negative IgG was performed to confirm

staining specificity (not shown). Magnification ×400. Quantification of AQP1 immunostaining is shown (**d**). Values are represented as mean±SEM. ***p*<0.01 and *****p*<0.0001 vs control and $^{\dagger\dagger\dagger\dagger}p$<0.0001 vs diabetic

Fig. 9 *EGFR* promoter binding activity and *Renilla* luciferase assay. Cells were exposed to control medium, pioglitazone (Piog; 10 μmol/l) or the more selective PPARγ agonist, L-805645 (8 μmol/l) for 24 h. (**a**) The ChIP assay was performed using the ChIP Kit according to the manufacturer's instructions. Real-time PCR was performed on purified DNA samples which were immunoprecipitated with PPARγ antibody. (**b**) Luciferase activity was measured using the *Renilla* Luciferase Assay System according to the manufacturer's instructions. Results are expressed as mean±SEM and shown as fold change compared with control. Three independent cell culture preparations were performed. **p*<0.05 vs control

Figure 1

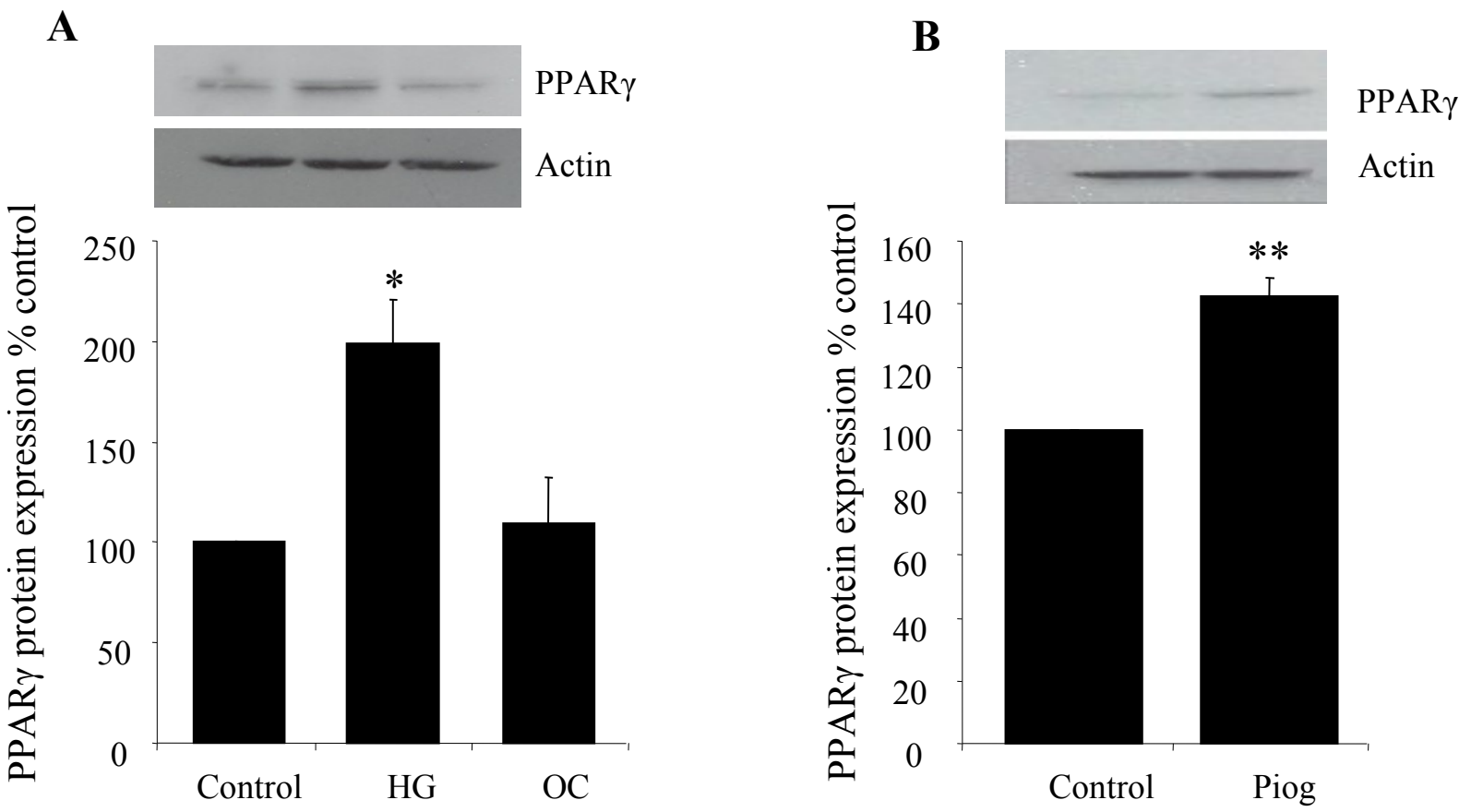
A
PPARγ
Actin
PPARγ protein expression % control
250
200
150
100
50
0
*
Control
HG
OC
B
PPARγ
Actin
PPARγ protein expression % control
160
140
120
100
80
60
40
20
0
**
Control
Piog

Figure 2

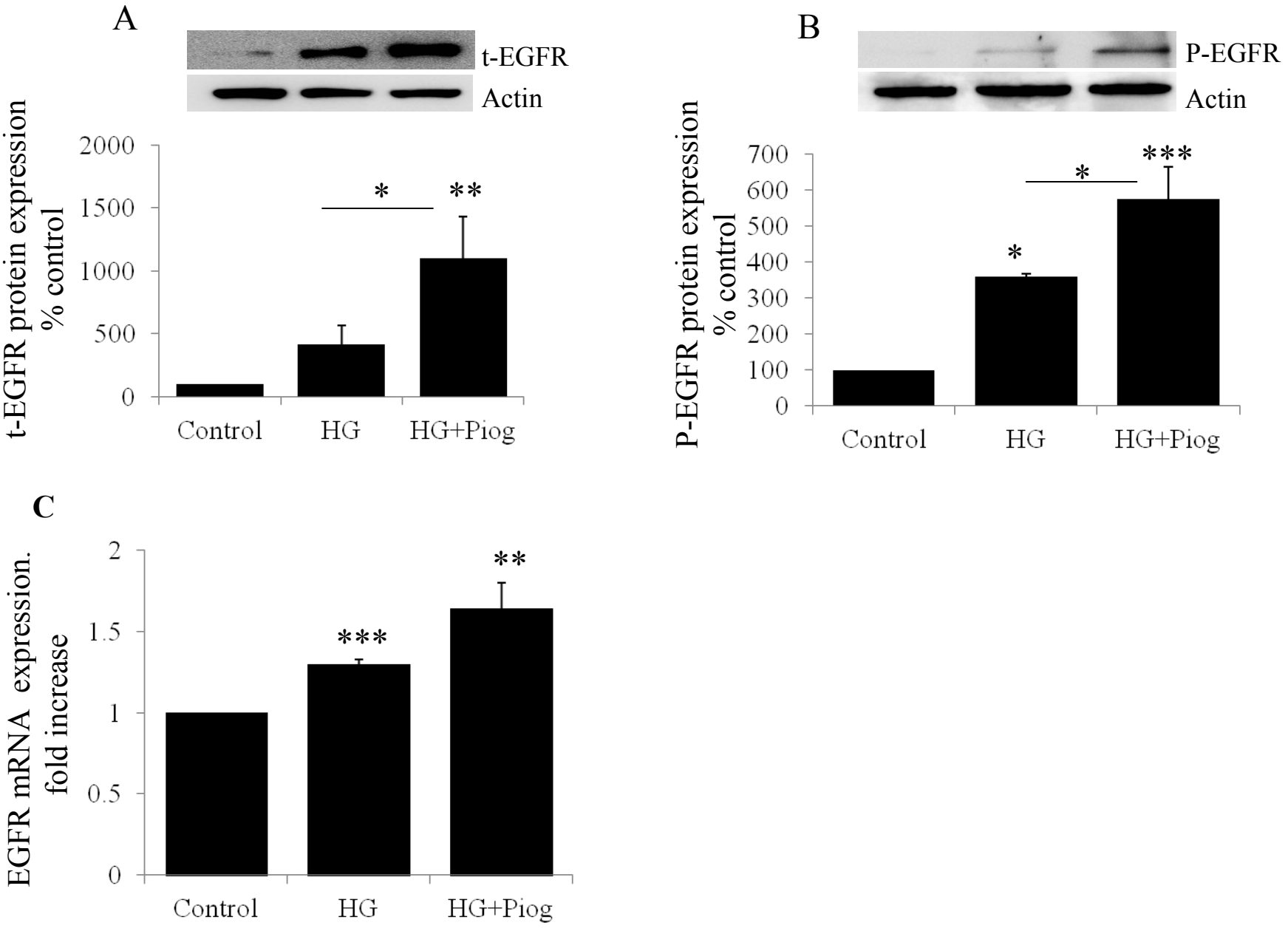
A
t-EGFR
Actin
t-EGFR protein expression
% control
2000
1500
1000
500
0
*
**
Control
HG
HG+Piog
B
P-EGFR
Actin
P-EGFR protein expression
% control
700
600
500
400
300
200
100
0
*
*
***
Control
HG
HG+Piog
C
EGFR mRNA expression.
fold increase
2
1.5
1
0.5
0
***
**
Control
HG
HG+Piog

Figure 3

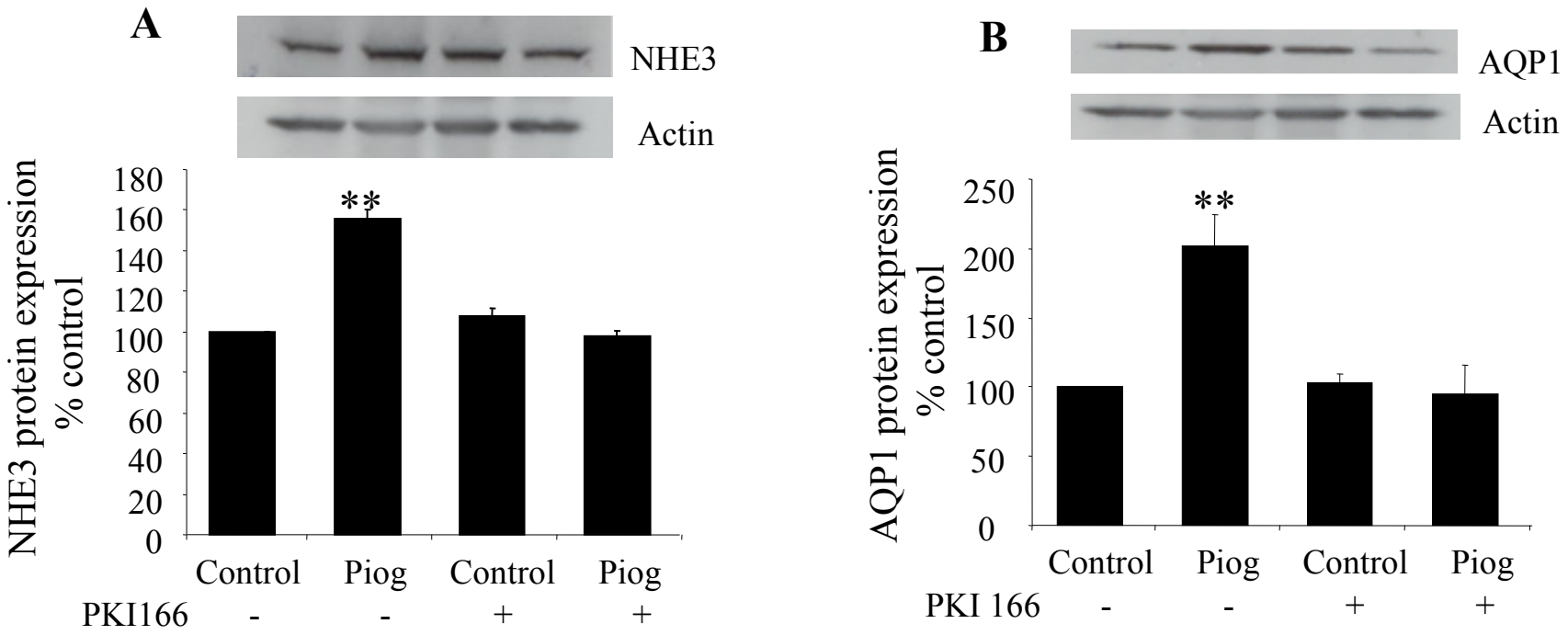
A
NHE3
Actin
NHE3 protein expression
% control
180
160
140
120
100
80
60
40
20
0
**
Control
Piog
Control
Piog
PKI166
-
-
+
+
B
AQP1
Actin
AQP1 protein expression
% control
250
200
150
100
50
0
**
Control
Piog
Control
Piog
PKI 166
-
-
+
+

Figure 4

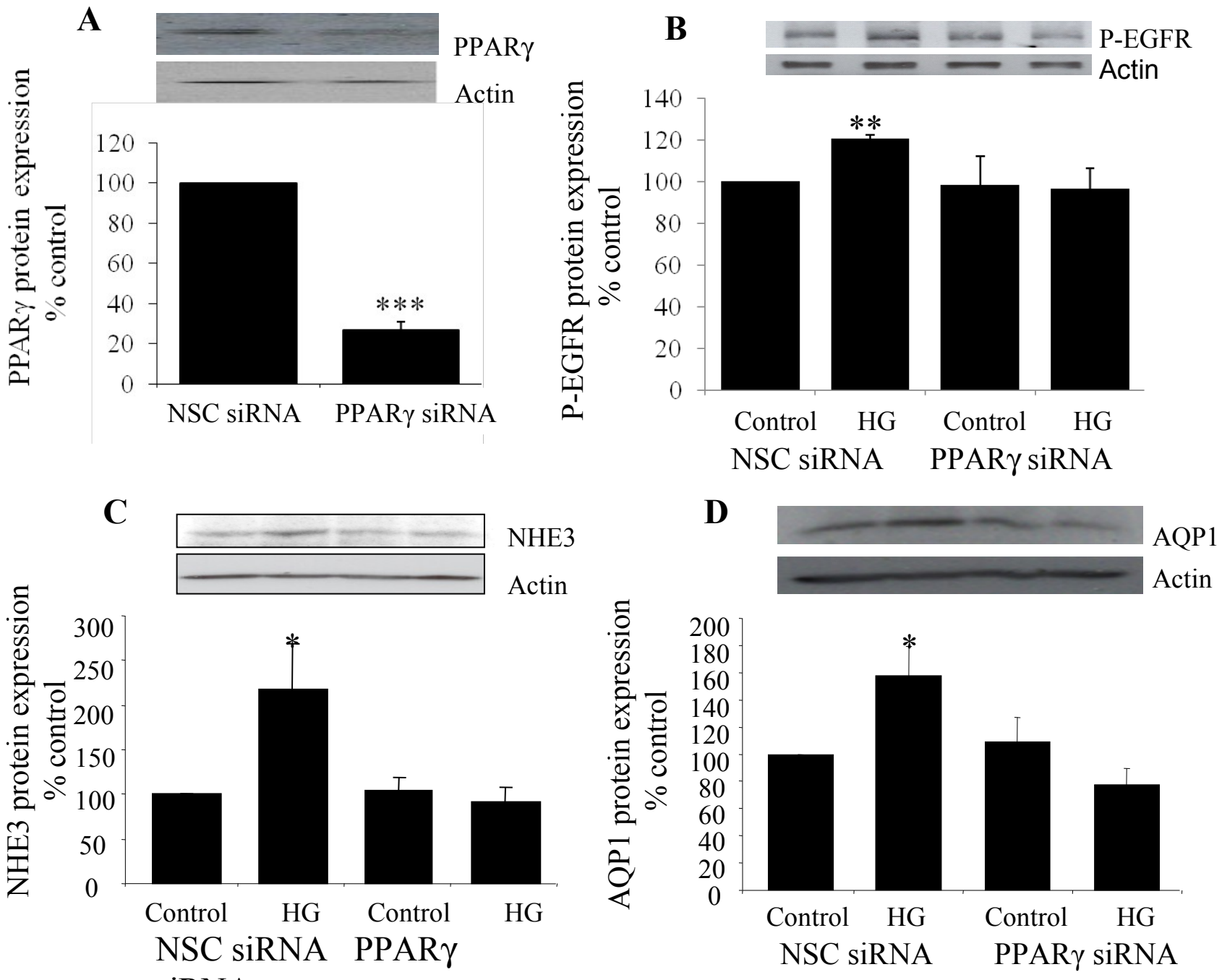
A
PPARγ
Actin
PPARγ protein expression
% control
120
100
80
60
40
20
0
***
NSC siRNA
PPARγ siRNA
B
P-EGFR
Actin
P-EGFR protein expression
% control
140
120
100
80
60
40
20
0
**
Control
HG
Control
HG
NSC siRNA
PPARγ siRNA
C
NHE3
Actin
NHE3 protein expression
% control
300
250
200
150
100
50
0
*
Control
HG
Control
HG
NSC siRNA
PPARγ
D
AQP1
Actin
AQP1 protein expression
% control
200
180
160
140
120
100
80
60
40
20
0
*
Control
HG
Control
HG
NSC siRNA
PPARγ siRNA

Figure 5

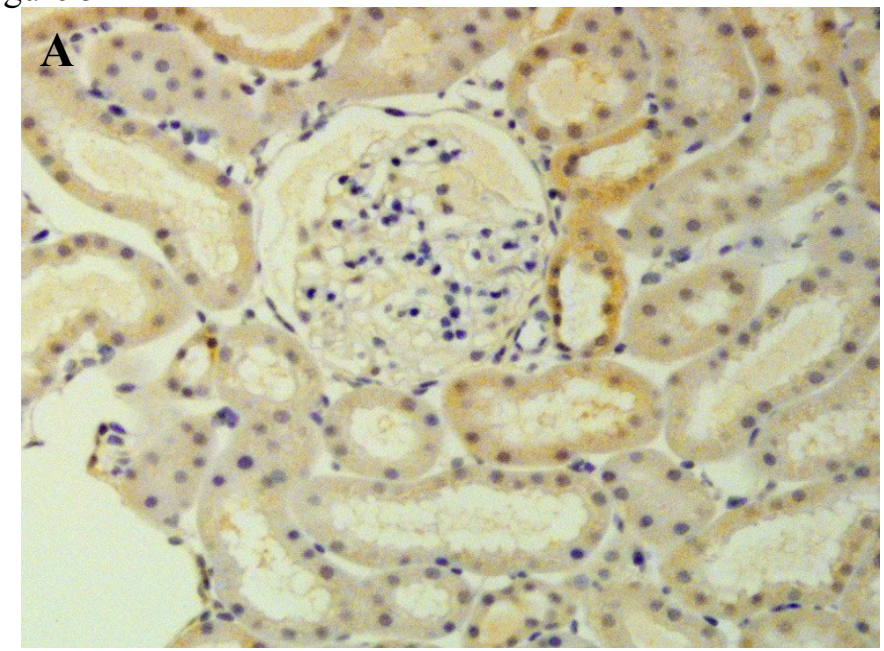
A

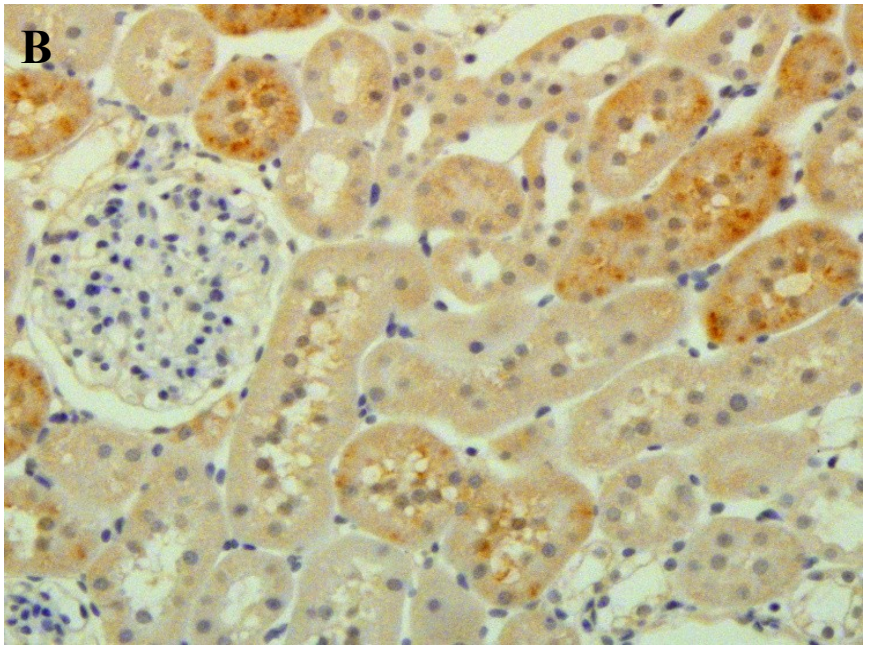
B

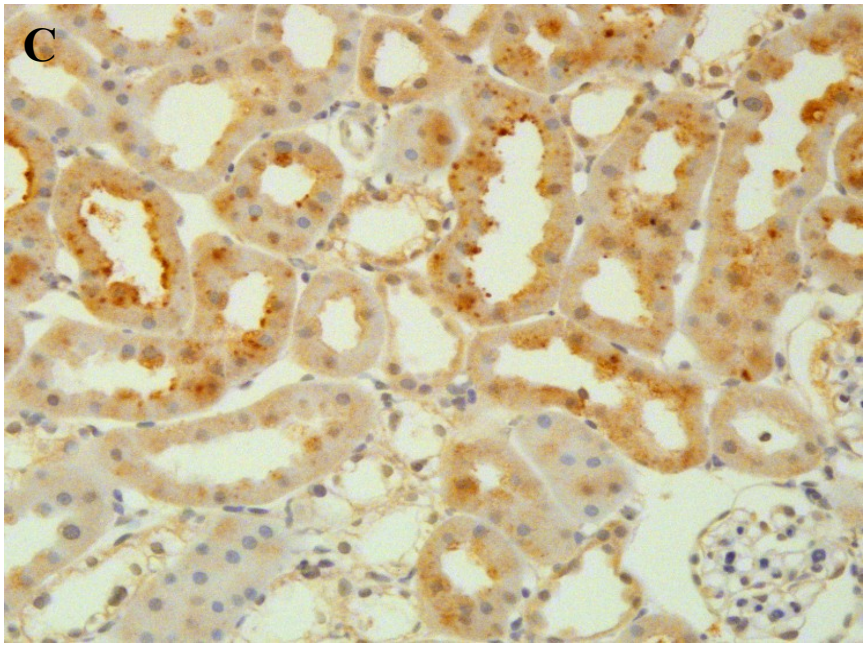
C

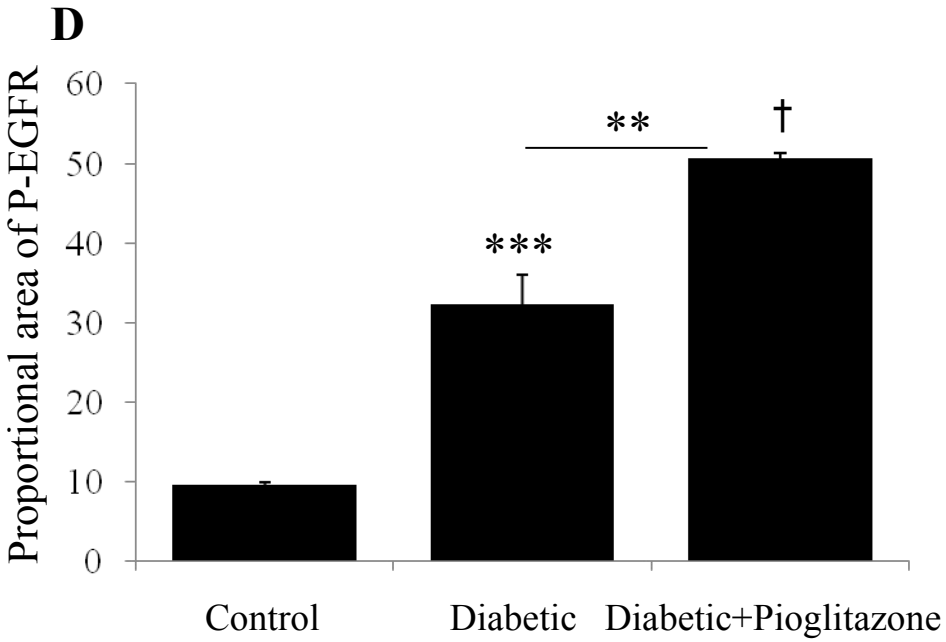
D
Proportional area of P-EGFR
60
50
40
30
20
10
0
**
†
***
Control
Diabetic
Diabetic+Pioglitazone

Figure 6

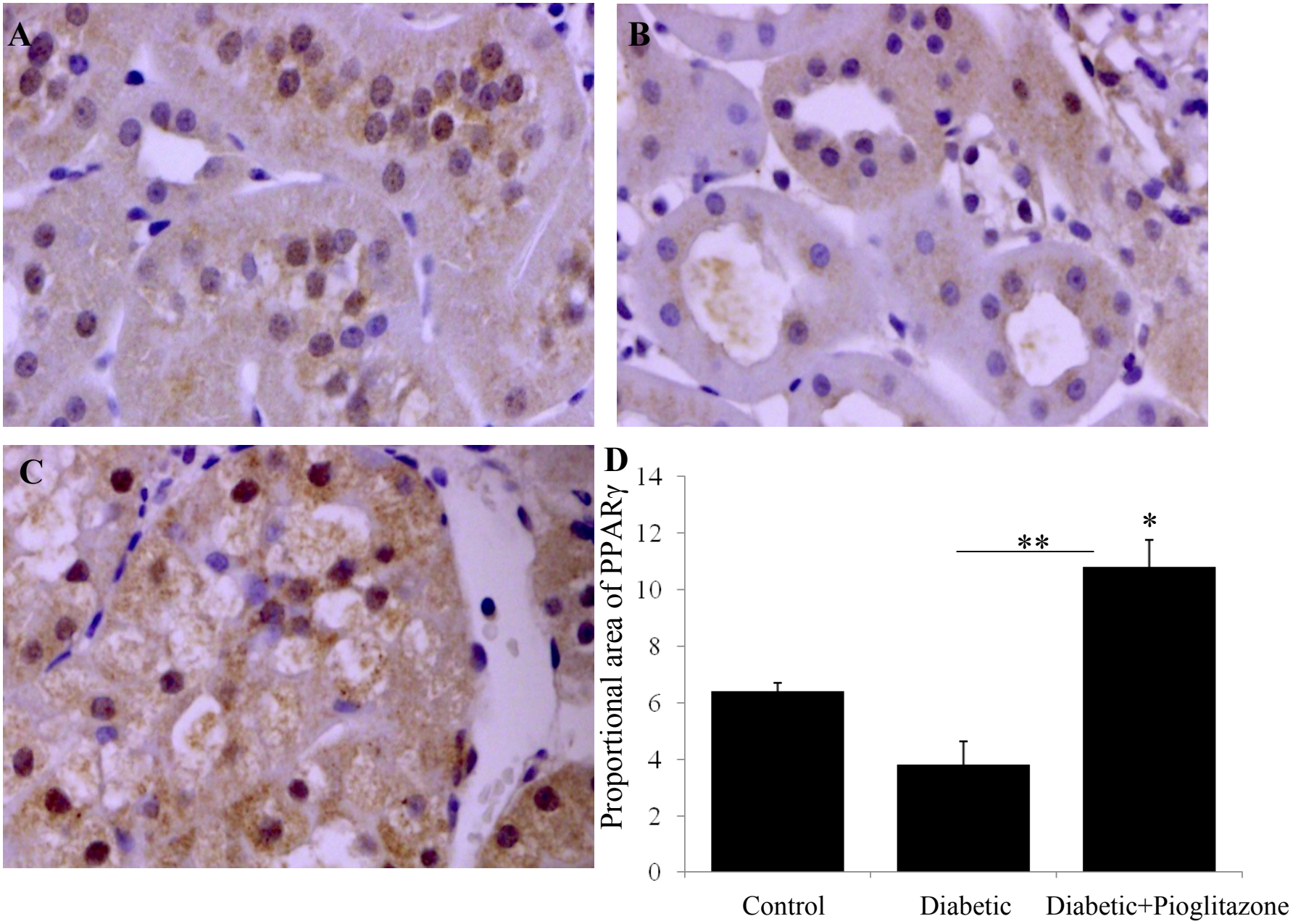
A
B
C
D
Proportional area of PPARγ
14
12
10
8
6
4
2
0
**
*
Control
Diabetic
Diabetic+Pioglitazone

Figure 7

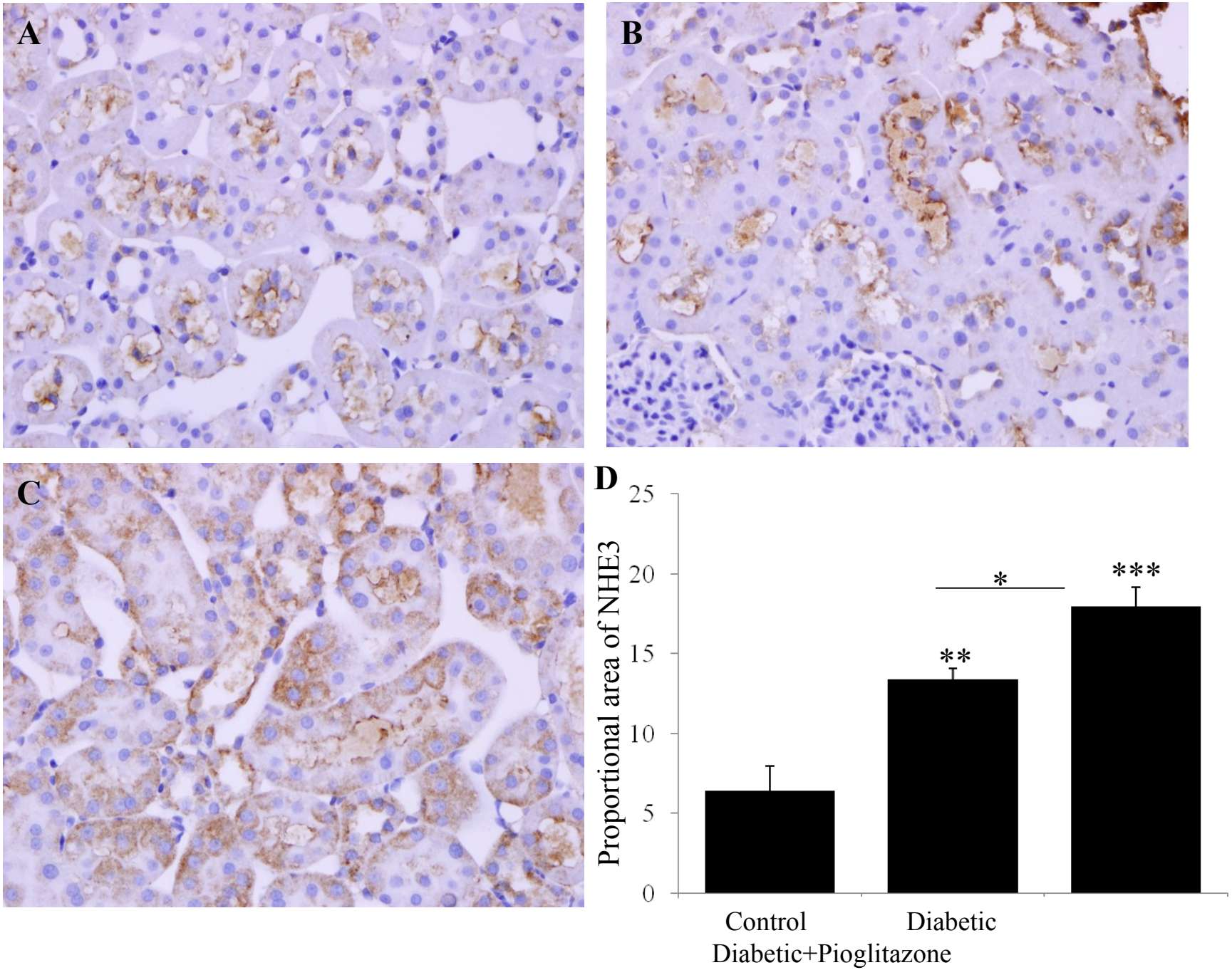
A
B
C
D
Proportional area of NHE3
25
20
15
10
5
0
*
**
***
Control
Diabetic
Diabetic+Pioglitazone

Figure 8

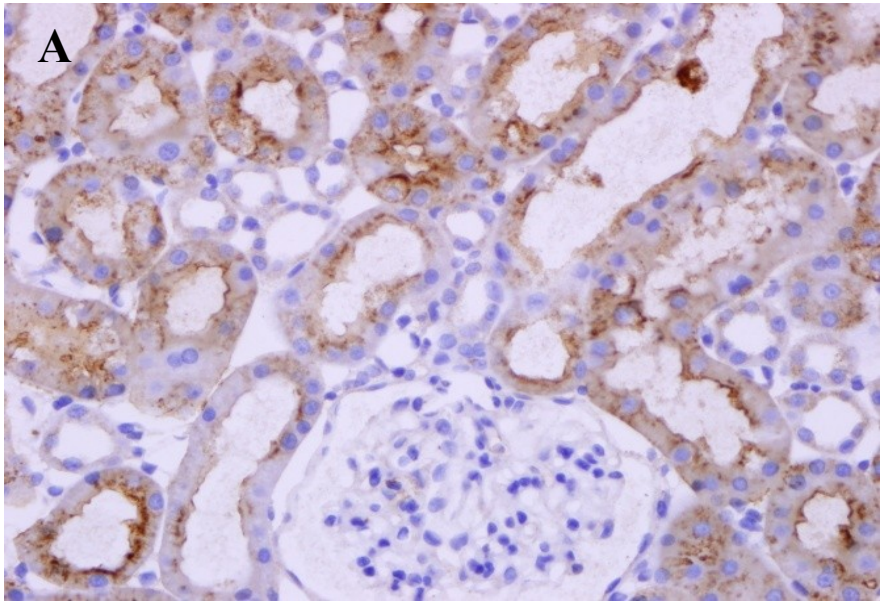
A

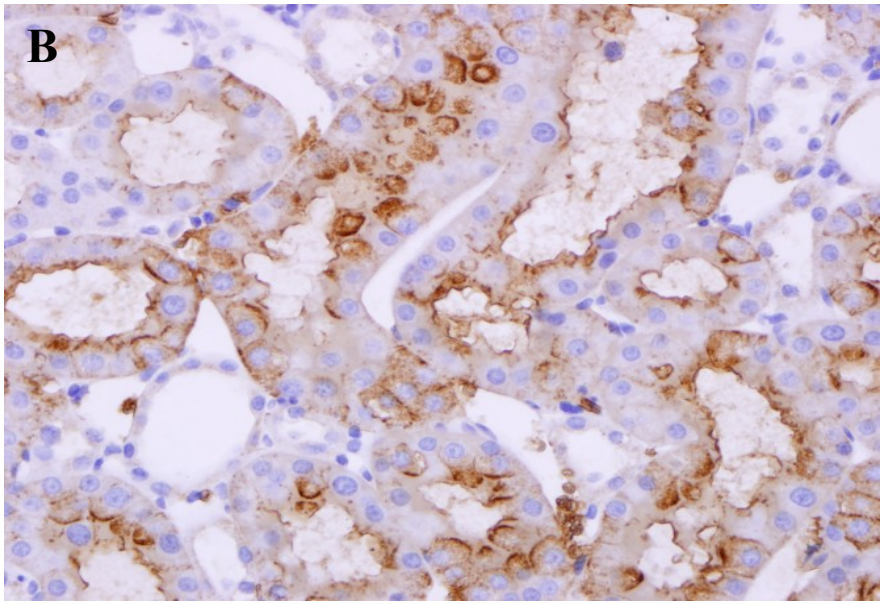
B

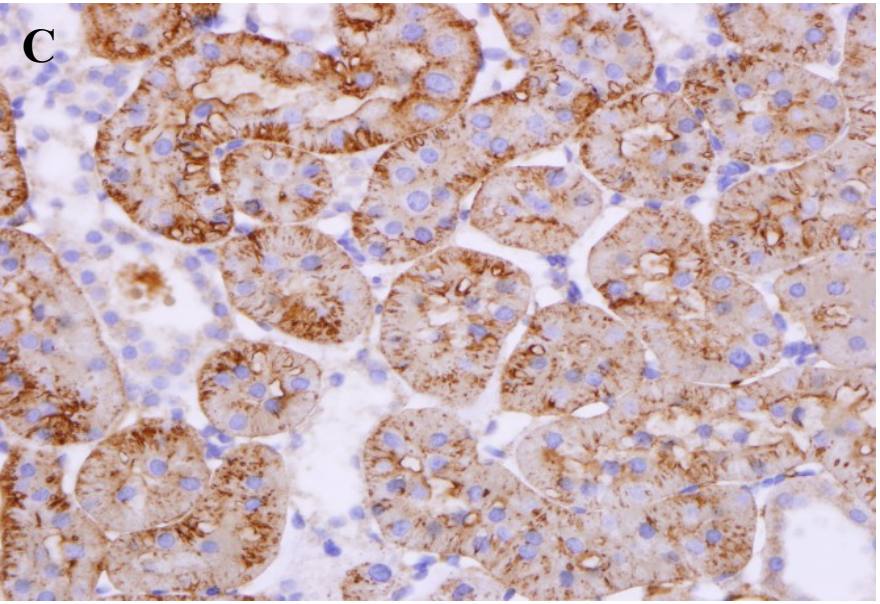
C

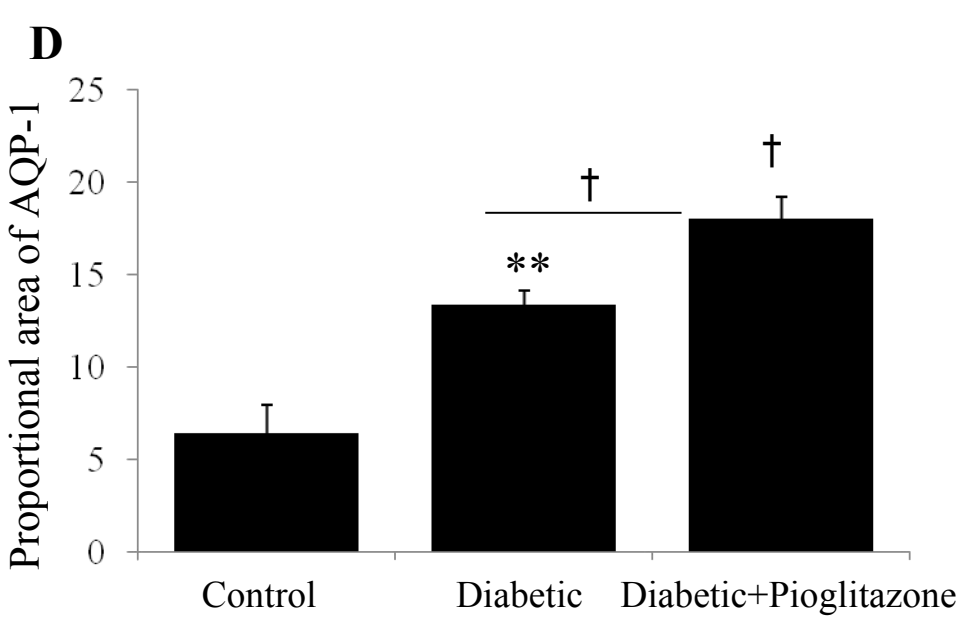
D
Proportional area of AQP-1
25
20
15
10
5
0
**
†
†
Control
Diabetic
Diabetic+Pioglitazone

Figure 9

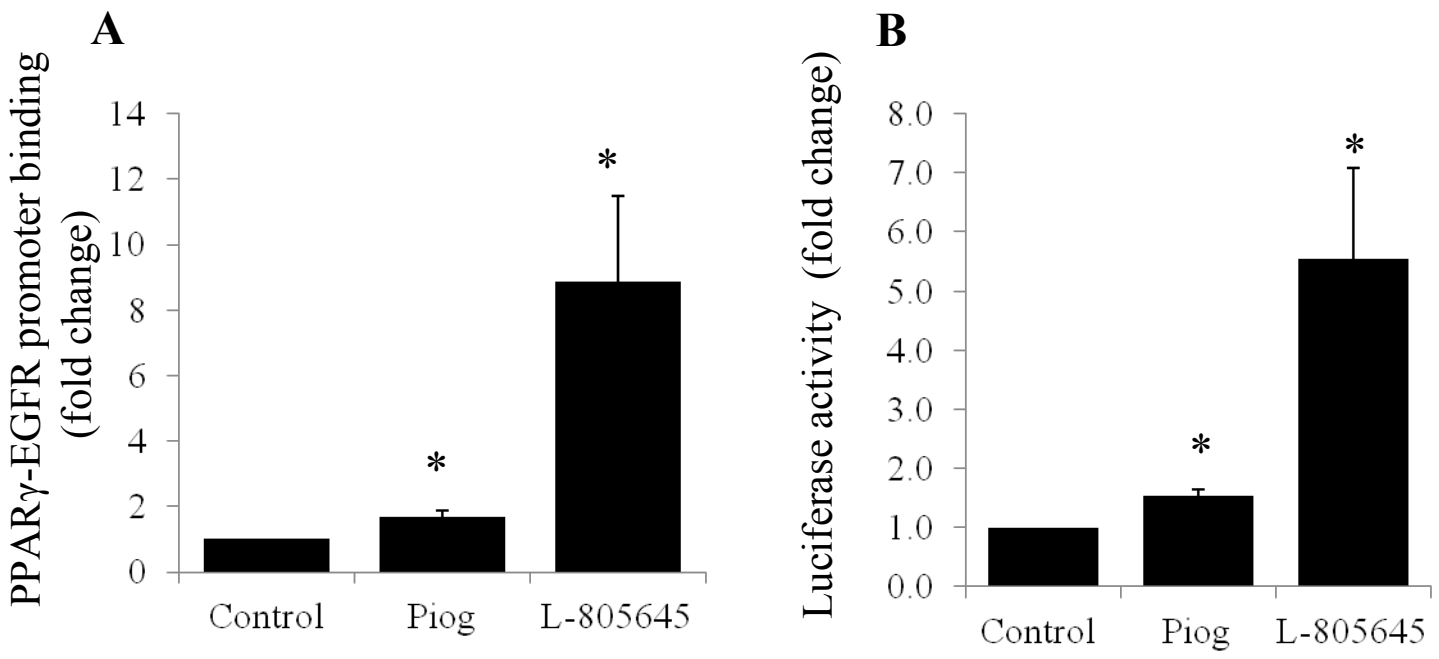
A
PPARγ-EGFR promoter binding (fold change)
14
12
10
8
6
4
2
0
*
*
Control
Piog
L-805645
B
Luciferase activity (fold change)
8.0
7.0
6.0
5.0
4.0
3.0
2.0
1.0
0.0
*
*
Control
Piog
L-805645

12 1732
Saad

Fig. 1

Global. Please change part labels to lower case
No bold except part labels

Please set in single column width.

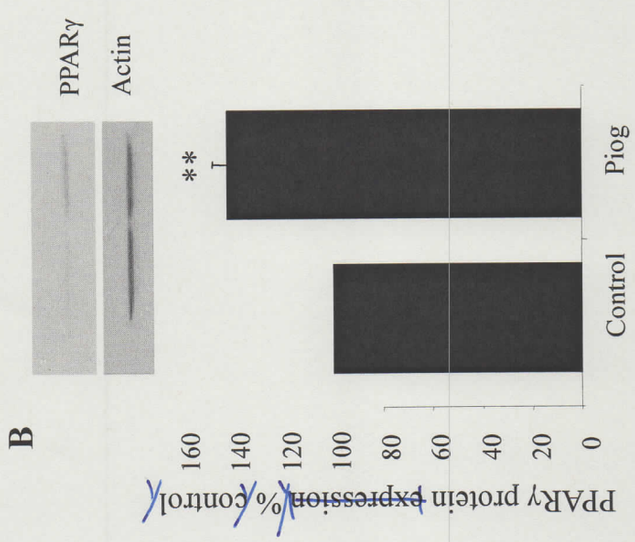

Level (% of control)

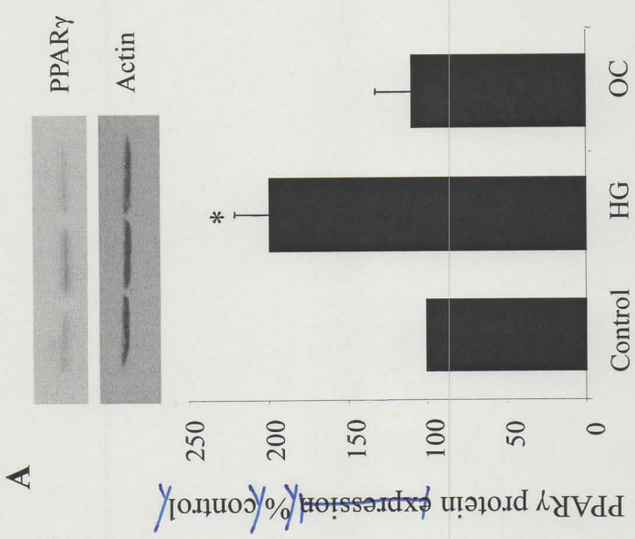

Level (% of control)

Figure 1

12 1732
Fig.2

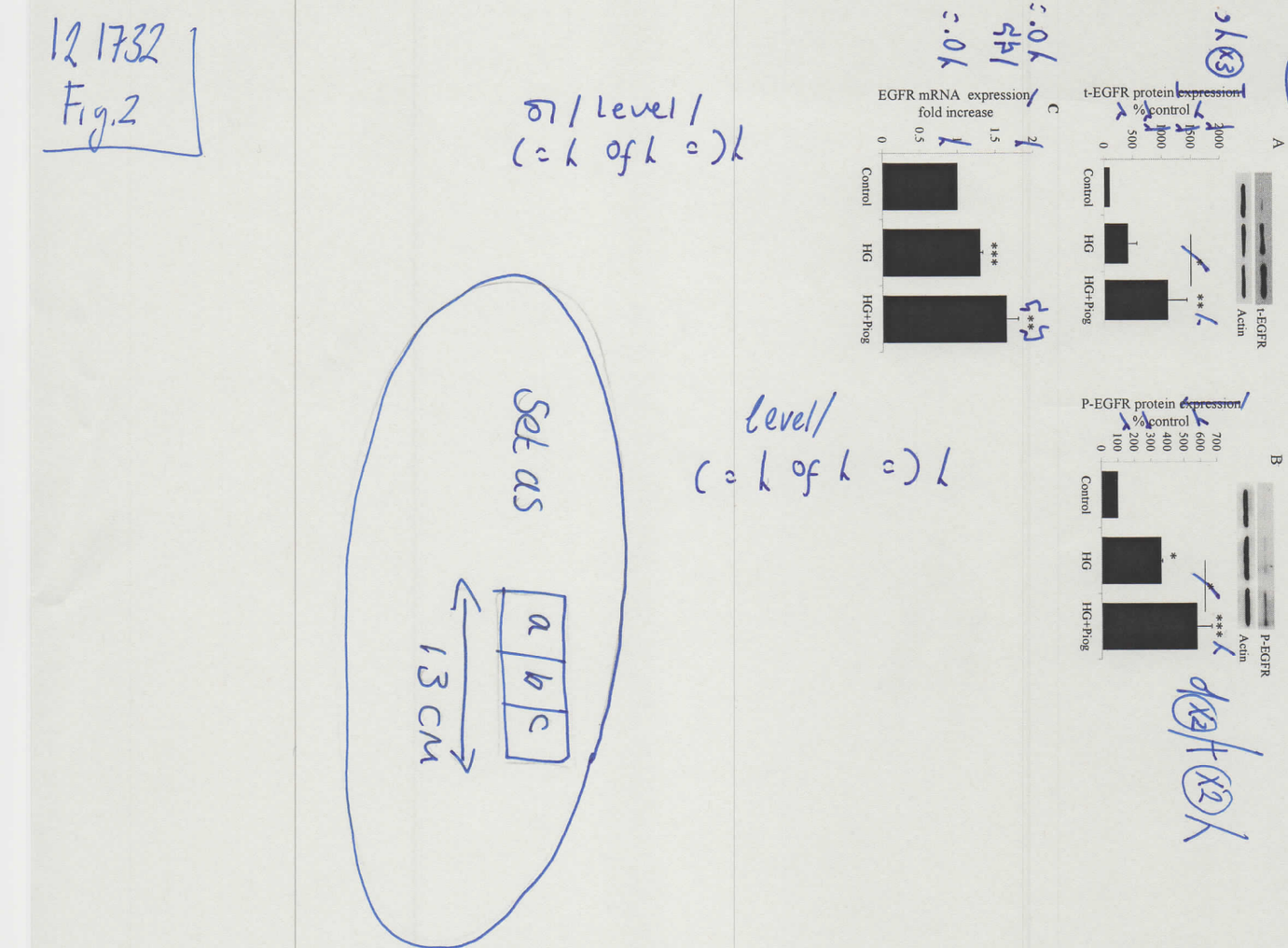
Figure 2
A
t-EGFR protein expression
% control
0
500
1000
1500
2000
Control
HG
HG+Prog
**
t-EGFR
Actin
B
P-EGFR protein expression
% control
0
100
200
300
400
500
600
700
Control
HG
HG+Prog
*
***
P-EGFR
Actin
C
EGFR mRNA expression
fold increase
0
0.5
1
1.5
2
Control
HG
HG+Prog
***
***

Set as
a
b
c
1.3 cm

121732
Fig. 3

level 1
(= L of L =)L

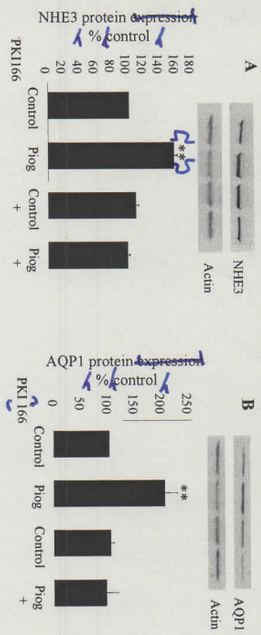

level 1
(= L of L =)L

Set in full column width.

12 1732
Fig 4

level / level / (= h of h =) h (= h of h =) h

level / level / (= h of h =) h (= h of h =) h

× Change to Times New Roman

— (×2) /

— (×4) /

Set in full column width

12732
Fig 5

Figure 5

Set in full column width

121732
Fig. 6

Figure 6

Set in full column width.

121732
Fig. 7

Set in full column width.

121732
Fig. 8

Figure 8

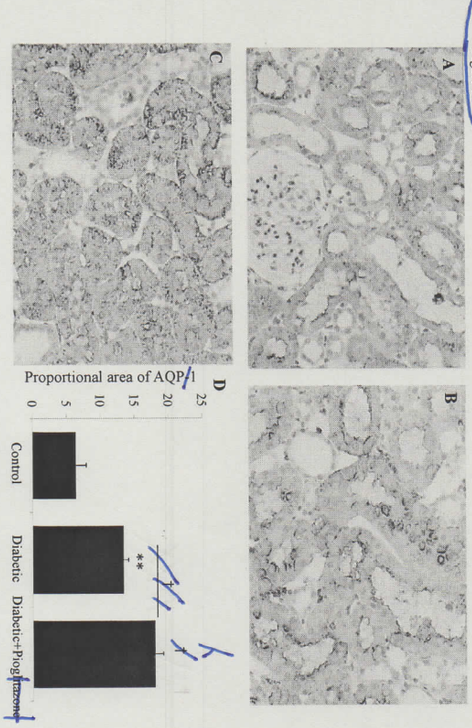

Set in full column width

12 1732

Fig. 9

IQ

1/

Figure 9

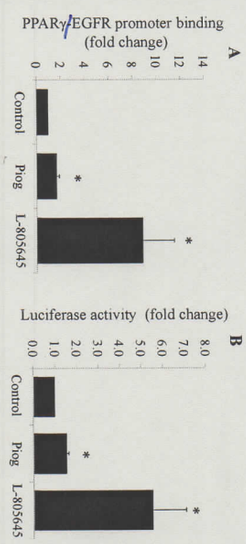

Set in full column width